Journal of Physics: Conference Series **436** (2013) 012023 doi:10.1088/1742-6596/436/1/012023

Symmetry-adapted *ab initio* no-core shell model calculations for ^{12}C

K D Launey[1], A C Dreyfuss[2], T Dytrych[1], J P Draayer[1], D Langr[3], P Maris[4], J P Vary[4], and C Bahri[5]

[1]Department of Physics and Astronomy, Louisiana State University, Baton Rouge, Louisiana 70803, USA
[2] Keene State College, Keene, New Hampshire 03435, USA
[3] Department of Computer Systems, Czech Technical University in Prague, Prague, Czech Republic
[4] Department of Physics and Astronomy, Iowa State University, Ames, Iowa 50011, USA
[5] Department of Physics, University of Notre Dame, Notre Dame, Indiana 46556, USA

E-mail: draayer@lsu.edu

Abstract. Symmetry-adapted no-core shell-model calculations reveal dominant symmetry patterns in the structure of light nuclei, independent of whether the system Hamiltonian is phenomenological in nature or derived from realistic interactions. We show results of large-scale nuclear structure computations based on the *ab initio* symmetry-adapted no-core shell model that use only a fraction of the model space. In addition, the symmetry patterns unveiled in these results are employed to explore ultra-large model spaces for ^{12}C. The outcome suggests a possible path forward for realizing collective theories that target correlated highly-deformed and alpha-cluster structures in terms of microscopic degrees of freedom that build forward from the nucleon-nucleon interaction itself.

1. Introduction

Complex nuclear systems often display striking simplicities. Experimental evidence supports the fact that low-lying nuclear states in light and medium-mass nuclei favor a dominance of low spin and high deformation, which has been also recently demonstrated through our first-principle studies [1, 2]. This, in turn, points to a remarkable new insight into the symmetry patterns observed in atomic nuclei, namely, understanding the mechanism on how such simple structures emerge from the fundamental level of the underlying quark/gluon physics.

The symmetry-guided approach we have developed utilizes symmetry to reduce the dimensionality of the model space through a very structured winnowing of the basis states to physically relevant subspaces. We achieve significantly enhanced reach beyond that of the current no-core shell model (NCSM) by taming the scale explosion problem through the development of a practical, *ab initio* symmetry-adapted no-core shell model (SA-NCSM) framework. This framework exploits our knowledge of dominant symmetries, first of the interaction itself and then of those that emerge as a result of the many-body dynamics, and utilizes the power of the current and unfolding next-generation of high performance computing (HPC) facilities. This combination opens up new regions of the periodic chart, the '*sd*-shell', to investigation with *ab initio* methods. Our approach enables the inclusion of higher-order correlations as required,

for example, for understanding excited 0^+ states – e.g., the elusive Hoyle state – in the lighter nuclei, and sets the stage for advancing the applicability of the current *ab initio* methods to systems beyond (e.g., 'fp-shell' nuclei, and even beyond to 'upper fp-shell' and 'lower gds-shell' as well as rare-earth and actinide species where deformation plays an even more dominant role) that are necessary, for example, for a better understanding of astrophysical processes among higher-mass nuclei.

The theory is applied to a study of the structure of ^{12}C, and in particular, to shape deformations and cluster substructures that are well pronounced in the low-lying states of this nucleus. Comparisons with results from conventional no-core shell model analyses illustrate the efficacy of the symmetry-adapted framework. In addition, a simple algebraic interaction, which reduces to the Elliott model in its single-shell limit, is shown to reproduce all features of the elusive Hoyle state in ^{12}C. While this requires that the no-core underpinning of the model be extended beyond the current reach of the standard no-core shell model to excitations as high as eighteen major oscillator shells, only the most deformed configurations in the extended region are required. This further affirms the importance of exploiting algebraic methods in exploring special correlations in many-particle and multi-shell environments.

2. Symmetry patterns revealed by the *ab initio* SA-NCSM model

The *ab initio* symmetry-adapted no-core shell model (SA-NCSM) [2] adopts the first-principle concept. The conventional NCSM basis spaces are constructed using harmonic oscillator (HO) single-particle states and are characterized by the $\hbar\Omega$ oscillator strength as well as by the cutoff in total oscillator quanta, $N_{\max}$, above the lowest energy configuration for a given nucleus. The basis states of the SA-NCSM for a given $N_{\max}$ are constructed in the proton-neutron formalism using also HO single-particle states and are labeled by the SU(3)$\supset$SO(3) subgroup chain quantum numbers $(\lambda\,\mu)\kappa L$, together with proton, neutron, and total intrinsic spins S_p, S_n, and S. The orbital angular momentum L is coupled with S to the total orbital momentum J and its projection M_J. Each basis state in this scheme is labeled schematically as $|\vec{\gamma}\,(\lambda\,\mu)\kappa L;(S_pS_n)S;JM_J\rangle$. The label κ distinguishes multiple occurrences of the same L value in the parent irrep $(\lambda\,\mu)$, and $\vec{\gamma}$ distinguishes among configurations carrying the same $(\lambda\,\mu)$ and $(S_pS_n)S$ labels.

The organization of the model space allows the full space to be down-selected to the physically relevant subspace [1, 3]. The significance of the SU(3) group for a microscopic description of the nuclear dynamics can be seen from the fact that it is the symmetry group of the Elliott model [4, 5, 6], and a subgroup of the Sp$(3,\mathbb{R})$, the underpinning symmetry of the symplectic model [7].

Ab initio SA-NCSM results for p-shell nuclei reveal a dominance of shapes of large deformation (typically large $|\lambda\ -\mu|$) in the $0\hbar\Omega$ subspace. For example, the *ab initio* SA-NCSM results with the bare JISP16 realistic interaction [8] for the 0^+ ground state (*g.st.*), first 2^+ and first 4^+ states of ^{12}C reveal the dominance of the $0\hbar\Omega$ component with the foremost contribution coming from the leading $(0\,4)$ $S=0$ irrep [9]. In addition, important SU(3) configurations are organized into structures with Sp$(3,\mathbb{R})$ symplectic symmetry, that is, the $(0\,4)$ symplectic irrep gives rise to $(0\,2)$ and $(2\,4)$ configurations in the $2\hbar\Omega$ subspace, and those configurations indeed realize the major components of the wavefunction in this subspace. This further confirms the significance of the symplectic symmetry to nuclear dynamics and points to the fact that the relevant model space can be systematically determined by down-selecting to important configurations (low-spin and high-deformation) in the high $N_{\max}$ spaces. This is illustrated in table 1, where results for the binding energy of ^{12}C and the point-particle matter rms radius of the ground state calculated in the symmetry-selected space of $N_{\max}=8[6]$ are compared to the corresponding counterparts calculated in the complete $N_{\max}=8$ space [10]. Here, the SA-NCSM basis space of $N_{\max}=8[6]$ (shown in fig. 1, filled circles) includes all the configurations up through $6\hbar\Omega$ (complete space,

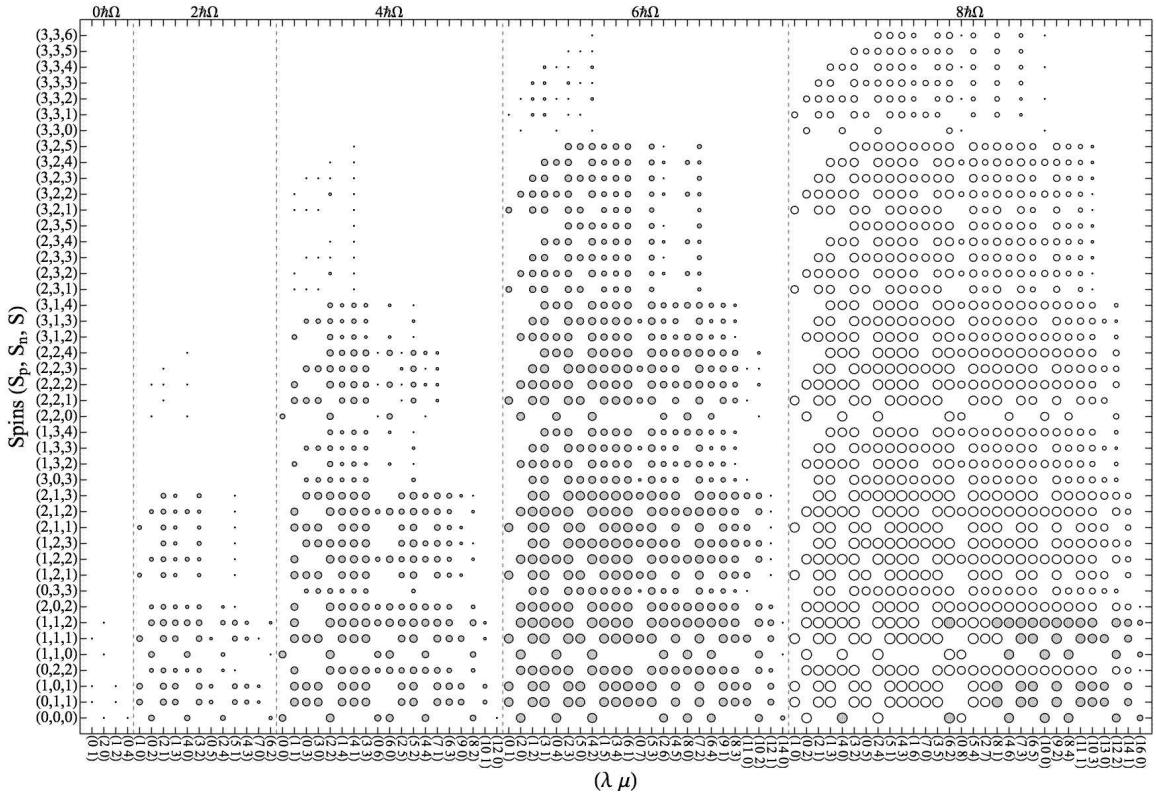

Figure 1. Complete $J = 0$ model space for ^{12}C and $N_{\max} = 8$ given in terms of spin values (vertical axis) and shapes (horizontal axis). Each circle represents basis states carrying the same (S_p, S_n, S) and $(\lambda\,\mu)$ quantum numbers within an $\hbar\Omega$-subspace, with the radius being proportional to $\log_{10}$ of the number of such states. Filled circles indicate the $N_{\max} = 8[6]$ restricted model space used in the present study for SA-NCSM calculations of 0^+ states in ^{12}C.

labeled as '[6]') and a restricted subspace thereof up to $N_{\max} = 8$.

The results clearly show that using only a 0.47% fraction of the complete $N_{\max} = 8$ model space, the $N_{\max} = 8[6]$ SA-NCSM outcome reproduces 98%-99% of the observables obtained in the complete $N_{\max} = 8$ space. This also holds for other observables, such as electric quadrupole moments and $B(E2)$ transition strengths [10]. While this simple example allows one to demonstrate the efficacy of the SA-NCSM as compared to the NCSM complexity, the significance of the SA-NCSM ability to drastically reduce the space dimensionality is critical for higher $N_{\max}$ spaces that are inaccessible to the NCSM.

3. Alpha-clustering phenomena described by the NCSpM model

The no-core symplectic shell model (NCSpM) is a fully microscopic no-core shell model that uses a symplectic $\mathrm{Sp}(3,\mathbb{R})$ basis and $\mathrm{Sp}(3,\mathbb{R})$-preserving interactions. The NCSpM employed within a full model space up through a given $N_{\max}$ coincides with the NCSM for the same $N_{\max}$ cutoff. However, in the case of the NCSpM, the symplectic irreps divide the space into 'vertical slices' that are comprised of basis states of a definite deformation $(\lambda\,\mu)$. Hence, the model space can be reduced to only a few important configurations that are chosen among all possible $\mathrm{Sp}(3,\mathbb{R})$ irreps within the $N_{\max}$ model space.

The NCSpM, while selecting the most relevant symplectic configurations, is employed to provide shell model calculations beyond current NCSM limits, namely, up through $N_{\max} = 20$

Table 1. ^{12}C binding energy and point-particle matter rms radius of the ground state for SA-NCSM reduced $N_{\max} = 8[6]$ and complete $N_{\max} = 8$ model spaces. The observables are calculated using bare JISP16 for $\hbar\Omega$=25 MeV and compared to experiment ('Expt.'). The fraction of the spaces used in the calculations as compared to the complete $N_{\max}$ space is also specified.

	$N_{\max} = 8[6]$	$N_{\max} = 8$	Expt.
Model space (%)	0.47% (J=0)	100%	
BE (MeV)	88.822	90.869	92.162
matter rms r (fm)	1.920	1.937	2.43(2)

for ^{12}C, the model spaces we found sufficient for the convergence of results [11]. We employ a very simple Hamiltonian with an effective interaction derived from the long-range expansion of the two-body central nuclear force,

$$H_{\rm eff} = H_0 - \frac{\chi}{2}\frac{1}{\gamma}\left(e^{\gamma(Q.Q-\langle Q.Q\rangle_n)} - 1\right), \quad (1)$$

which includes the spherical HO potential (which together with the kinetic energy yields the HO Hamiltonian, H_0) and the $Q.Q$ quadrupole-quadrupole interaction not restricted to a single shell. For the latter term, the average contribution, $\langle Q.Q\rangle_n$, of $Q.Q$ within a subspace of n HO excitations is removed [12]. Here, $\langle Q.Q\rangle_n$ is the trace of $Q.Q$ divided by the space dimension for a fixed n. Hence, the large monopole contribution of the $Q.Q$ interaction is removed, which, in turn, helps eliminate the spurious renormalization of the zero-point energy, while retaining the $Q.Q$-driven behavior of the wavefunctions.

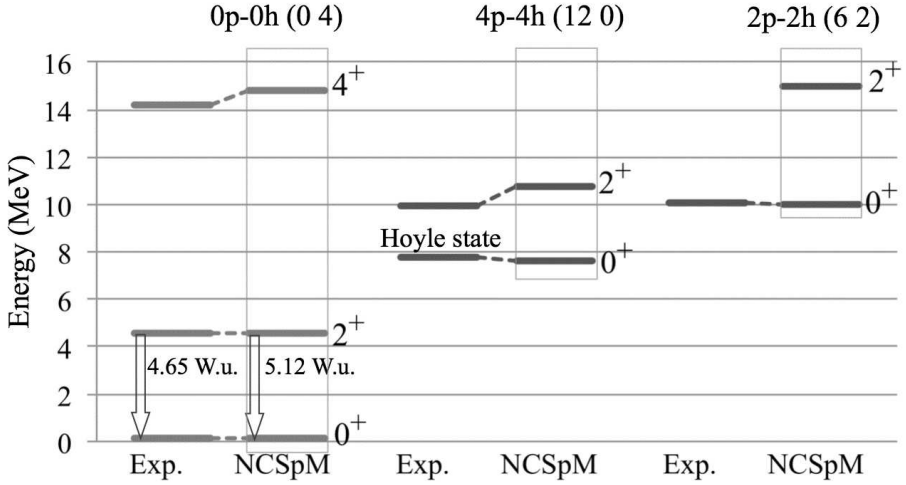

Figure 2. ^{12}C energy spectrum calculated by the $N_{\max} = 20$ NCSpM and compared to experiment. The NCSpM calculations are performed using eq. (1) with $\gamma = -1.71 \times 10^{-4}$ and three Sp$(3,\mathbb{R})$ irreps, $0\hbar\Omega$ 0p-0h (0 4) and $4\hbar\Omega$ 4p-4h (12 0), as well as $2\hbar\Omega$ 2p-2h (6 2). Experimental energies for all states, except the latest results for the 10-MeV 2^+ and 0^+_3 [13], are from [14].

This Hamiltonian in its zeroth-order approximation (for parameter $\gamma \to 0$) and for a single valence shell goes back to the established Elliott model [4, 6]. We take the coupling constant

χ to be proportional to $\hbar\Omega$ and, to leading order, to decrease with the total number of HO excitations, as shown by Rowe [15] based on self-consistent arguments. It is important to note that such a choice for χ renders the eigenstates $\hbar\Omega$-independent.

As the interaction and the model space are carefully selected to reflect the most relevant physics, the outcome reveals a quite remarkable agreement with experiment. The low-lying energy spectrum and eigenstates for ^{12}C were calculated using the NCSpM with H of eq. (1) for $\hbar\Omega = 18$ MeV given by the empirical estimate $\approx 41/A^{1/3} = 17.9$ MeV. The results are shown for $N_{\max} = 20$, which we found sufficient to yield convergence. This $N_{\max}$ model space is further reduced by selecting the most relevant symplectic irreps, namely, the spin-zero ($S = 0$) $0\hbar\Omega$ 0p-0h $(0\,4)$, $2\hbar\Omega$ 2p-2h $(6\,2)$, and $4\hbar\Omega$ 4p-4h $(12\,0)$ symplectic bandheads together with all multiples thereof up through $N_{\max} = 20$ of total dimensionality of 4.5×10^3. In comparison to the experimental energy spectrum (fig. 2), the outcome reveals that the lowest 0^+, 2^+, and 4^+ states of the $0\hbar\Omega$ 0p-0h $(0\,4)$ symplectic irrep calculated for $\gamma = -1.71 \times 10^{-4}$ closely reproduce the *g.st.* rotational band, while the calculated lowest 0^+ states of the $4\hbar\Omega$ 4p-4h $(12\,0)$ and the $2\hbar\Omega$ 2p-2h $(6\,2)$ slices are found to lie close to the Hoyle state and the 10-MeV 0^+ resonance (third 0^+ state), respectively. We note that the NCSpM energies given in fig. 2 are rescaled by an overall factor of ~ 2. This factor is determined by fixing the lowest 2^+ by its experimental value. This, however, has no implications on the underlying physics, as an overall factor for H does not change its properties and eigenstates, together with associated observables. Indeed, the model successfully reproduces other observables for ^{12}C that are informative of the state structure, such as matter rms radii, electric quadrupole moments and $B(E2)$ transition strengths. These quantities are shown in fig. 3, where the values obtained for $\gamma = -1.71 \times 10^{-4}$ lie remarkably close to the experimental data.

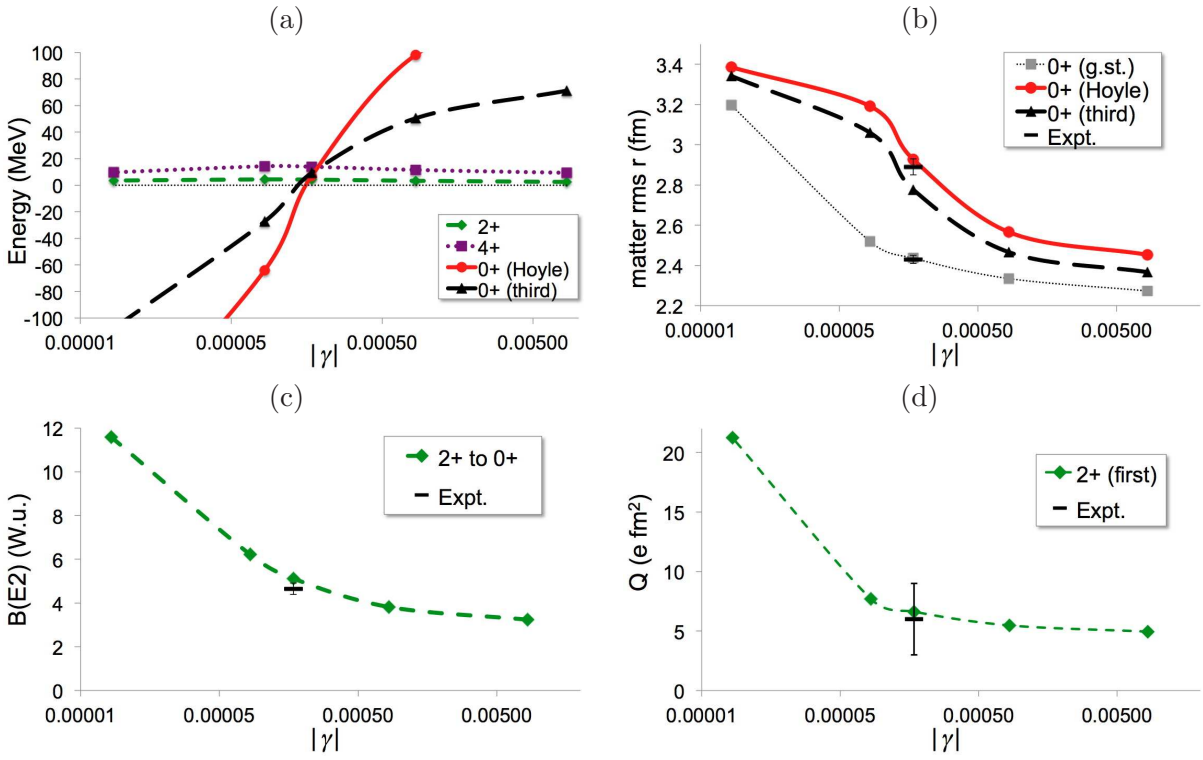

Figure 3. Dependence of the ^{12}C NCSpM energy spectrum on the γ model parameter for $N_{\max} = 20$. Available experimental values are shown for (b), (c), and (d) and compared to the NCSpM results with $\gamma = -1.71 \times 10^{-4}$.

Furthermore, fig. 3 reveals that the additional degree of freedom associated with the γ model parameter is in fact substantially limited by the lowest 0^+ states (with only a small effect on the *g.st.* rotational band). Clearly, while the model includes an adjustable parameter, γ only controls the decrease rate of the $Q.Q$ interaction with increasing n; the entire many-body apparatus is fully microscopic and no adjustments are possible. Hence, given the dramatic variation with γ of the energy and the relative position of the three lowest 0^+ states (including the *g.st.*), there is only a small window of reasonable γ values where observables are also found in agreement with experiment.

Table 2. Probability distribution for ^{12}C ($\geq 0.1\%$) over the n total excitations and the SU(3) $(\lambda\,\mu)$ of the lowest 0^+, 2^+, and 4^+ states as calculated by the NCSpM and by the *ab initio* SA-NCSM using the bare JISP16 for $\hbar\Omega = 20$ MeV and an $N_{\max} = 8$ $S_{p,n} = 0$ space.

0^+			2^+			4^+		
$n(\lambda\,\mu)$	Probability (%)		$n(\lambda\,\mu)$	Probability (%)		$n(\lambda\,\mu)$	Probability (%)	
	SA-NCSM	NCSpM		SA-NCSM	NCSpM		SA-NCSM	NCSpM
0 (0 4)	69.12	64.49	0 (0 4)	68.17	64.82	0 (0 4)	66.11	65.02
0 (2 0)	0.13		2 (2 4)	8.40	17.71	2 (2 4)	9.26	17.84
2 (2 4)	8.35	17.85	2 (0 2)	4.58	0.68	2 (1 3)	8.60	0.3
2 (0 2)	7.07	0.95	2 (1 3)	3.41		2 (6 2)	0.76	
2 (6 2)	1.82		2 (6 2)	1.48		2 (4 3)	0.16	
4 (4 4)	6.34	9.44	4 (4 4)	6.25	9.24	4 (4 4)	6.08	8.98
4 (2 2)	1.56	0.98	4 (2 2)	0.91	0.76	4 (3 3)	1.86	0.11
4 (0 0)	0.55		4 (1 1)	0.84		4 (2 2)	1.35	0.18
4 (8 2)	0.54		4 (3 3)	0.61		4 (1 4)	0.35	1.19
4 (0 6)	0.23	0.67	4 (8 2)	0.45		4 (0 6)	0.31	0.37
4 (6 0)	0.16		4 (0 6)	0.25	0.58	4 (8 2)	0.30	
6 (6 4)	1.50	3.22	4 (1 4)	0.16	0.32	6 (6 4)	1.39	3.22
6 (4 2)	0.63	0.32	4 (5 2)	0.11		6 (5 3)	0.49	
6 (2 6)	0.31	0.11	6 (6 4)	1.45	3.18	6 (2 6)	0.33	
6 (10 2)	0.20		6 (4 2)	0.42	0.18	6 (3 4)	0.29	0.37
6 (2 0)	0.18		6 (2 6)	0.31		6 (4 2)	0.26	
8 (8 4)	0.51	1.1	6 (5 3)	0.18		6 (10 2)	0.11	
8 (6 2)	0.20	0.12	6 (10 2)	0.16		6 (3 1)	0.11	
8 (4 6)	0.14		6 (3 1)	0.14		8 (8 4)	0.47	1.08
10 (10 4)	—	0.32	6 (3 4)	0.12		8 (7 3)	0.21	
			8 (8 4)	0.50	1.09	8 (4 6)	0.13	
			8 (4 6)	0.13		8 (5 4)		0.16
			8 (6 2)	0.13		10 (10 4)	—	0.28
			10 (10 4)	—	0.25			

In addition, a close similarity is observed when the probability distributions for the *g.st.* rotational band are compared to *ab initio* results when only configurations of zero proton and neutron spins ($S_{p,n} = 0$) are selected (table 2). In particular, NCSpM eigenstates, which are $\hbar\Omega$-independent, are compared to SA-NCSM calculations with the bare JISP16 realistic interaction for $\hbar\Omega = 20$ MeV (around the minimum of the calculated binding energy for ^{12}C) and a $N_{\max} = 8$ model space. This space appears to be sufficient to yield convergent results for the *g.st.* rotational

band for both models. The close agreement points to the fact that the schematic interaction used in NCSpM has effectively captured most of the underlying physics of the realistic interaction important to the low-energy nuclear dynamics.

Furthermore, in accordance with the mapping [16] between the shell-model $(\lambda\,\mu)$ SU(3) labels and the shape variables of the Bohr-Mottelson collective model [17], the symplectic basis states bring forward important information about the nuclear shapes and deformation. The simplest cases, $(0\,0)$, $(\lambda\,0)$, and $(0\,\mu)$, describe a spherical, prolate, and oblate shape, respectively, while a general nuclear state is typically a superposition of several hundred various triaxial shapes. Thus, while a preponderance of the $(0\,4)$ shape (of $\sim 65\%$ probability) is observed for the *g.st.* rotational band (table 2), indicating a pronounced oblate shape of the *g.st.*, the $(12\,0)$ bandhead of the Hoyle-state rotational band includes shapes of even larger deformations (more prolate) with the largest contribution ($\sim 30\%$) of $(16\,0)$.

4. Conclusion

We showed that employing the symmetry-adapted no-core shell-model with SU(3) the underpinning symmetry is effective in providing an efficient description of low-lying eigenstates of ^{12}C, which also holds for various other p-shell nuclei. The symmetry patterns revealed in the *ab initio* calculations were, in turn, employed to reach ultra-large model spaces that are currently inaccessible. We carried forward a no-core shell-model study with a schematic many-nucleon interaction to further unveil the underlying physics behind various phenomena important to the low-energy nuclear dynamics of ^{12}C. We showed, for the first time, how both collective and cluster-like structures emerge out of a shell-model framework, which can extend to and take into account essential high-lying configurations.

Acknowledgments

We thank all members of the NSF PetaApps supported collaboration for useful discussions. This work was supported by the U.S. NSF (OCI-0904874 & OCI-0904782), the U.S. DOE (DE-SC0005248, DE-FG02-95ER-40934, DE-SC0008485 & DE-FG02-87ER40371), and SURA. ACD acknowledges support by the U.S. NSF (grant 1004822) through the REU Site in Dept. of Physics & Astronomy at LSU. We acknowledge LSU/LONI for providing HPC resources. A portion of the computational resources were provided by the NERSC Center, which is supported by the Office of Science of the U.S. DOE under Contract DE-AC02-05CH11231.

References

[1] Dytrych T, Sviratcheva K D, Bahri C, Draayer J P and Vary J P 2007 *Phys. Rev. Lett.* **98** 162503
[2] Dytrych T *et al.* 2013 *to be submitted to Phys. Rev. Lett.*
[3] Dytrych T, Sviratcheva K D, Draayer J P, Bahri C and Vary J P 2008 *J. Phys. G: Nucl. Part. Phys.* **35** 123101
[4] Elliott J P 1958 *Proc. Roy. Soc. A* **245** 128
[5] Elliott J P 1958 *Proc. Roy. Soc. A* **245** 562
[6] Elliott J P and Harvey M 1962 *Proc. Roy. Soc. A* **272** 557
[7] Rosensteel G and Rowe D J 1977 *Phys. Rev. Lett.* **38** 10
[8] Shirokov A M, Vary J P, Mazur A I and Weber T A 2007 *Phys. Lett.* **B 644** 33
[9] Draayer J P, Dytrych T, Launey K D and Langr D 2012 *Prog. Part. Nucl. Phys.* **67** 515
[10] Dytrych T, Maris P, Launey K D, Draayer J P, Vary J P, Caprio M A, Langr D, Çatalyürek Ü V, Saule E and Sosonkina M 2013 *to be submitted*
[11] Dreyfuss A C, Launey K D, Dytrych T, Draayer J P and Bahri C 2012 *Preprint* arXiv:1212.2255
[12] Rosensteel G and Draayer J P 1985 *Nucl. Phys. A* **436** 445
[13] Itoh M *et al.* 2011 *Phys. Rev. C* **84** 054308
[14] Ajzenberg-Selove F 1990 *Nucl. Phys. A* **506** 1
[15] Rowe D J 1967 *Phys. Rev.* **162** 866
[16] Castaños O, Draayer J P and Leschber Y 1988 *Z. Phys. A* **329** 33
[17] Bohr A and Mottelson B R 1969 vol 1 (New York: Benjamin)